Collisional-radiative model for lithiumlike ions in plasma

Tetsuya Kawachi and Takashi Fujimoto
Department of Engineering Science, Kyoto University, Kyoto 606-01, Japan

George Csanak
Los Alamos National Laboratory, Los Alamos, New Mexico 87540
(Received 25 April 1994)

For low-lying levels with principal quantum number $n \leq 5$, different l levels are treated separately and the fine structure is taken into account, where l is the orbital angular momentum. The electron impact excitation cross section of an oxygen ion (O VI) is calculated for virtually all the transitions among the $n \leq 5$ levels and it is scaled for other elements. The calculated populations of excited levels and the effective ionization rate coefficient are favorably compared with available experimental results.

PACS number(s): 52.70.−m

I. INTRODUCTION

Lithiumlike ions play an important role in the spectroscopy of laboratory and astrophysical plasmas. In tokamak plasmas, for example, prominent impurity lines are emitted by lithiumlike ions of oxygen, carbon, and other elements. Determination of the absolute density of these ions for the purpose of studying their transport is one of the subjects of tokamak plasma spectroscopy. Recently an x-ray laser based on the recombining lithiumlike ion scheme has been extensively studied. For the purpose of evaluating the ground-state ion density in the former plasma, and studying the population inversion and gain in the latter plasma, a reliable collisional-radiative (CR) model is indispensable. Klisnick *et al.* [1] first constructed a CR model for lithiumlike aluminum ions. The cross section data in their model, however, are rather unsophisticated, and the model has been applied only to the low temperature recombining plasma.

In the following, we describe our collisional-radiative model with the fine structure taken into account. We examine the atomic data in Sec. III. A comparison of the result with the available plasma experiments is made in Sec. IV. The uncertainties in and the validity range of our model are discussed in Sec. V.

II. COLLISIONAL-RADIATIVE MODEL

The temporal development of population $n(p)$ of level p of ions in plasma is expressed by the differential equation

$$\frac{dn(p)}{dt}=\sum_{q<p} C(q,p)n_e n(q)-\left\{\left[\sum_{q<p} F(p,q)+\sum_{q>p} C(p,q)\right]n_e+\sum_{q<p} A(p,q)\right\}n(p)$$
$$+\sum_{q>p}[F(q,p)n_e+A(q,p)]n(q)-S(p)n_e n(p)+[\alpha(p)n_e+\beta(p)+\gamma(p)]n_e n_{\mathrm{He}}\ , \tag{1}$$

which is coupled with similar equations for other levels. Here $q<p$ means that level q lies energetically lower than level p. $A(p,q)$ is the spontaneous transition probability from p to q, $C(p,q)$, $F(q,p)$, and $S(p)$ are the rate coefficients for electron impact excitation, deexcitation, and ionization, respectively, and $\alpha(p)$, $\beta(p)$, and $\gamma(p)$ are the rate coefficients for three-body, radiative and dielectronic recombination, respectively. n_e is the electron density, and we express the ground-state heliumlike ion density as n_{He}. We have assumed that the excited ions are created starting from the ground-state lithiumlike ions or heliumlike ions; i.e., we ignore the direct populating processes of lithiumlike excited levels from the lower ionization stage ions like berylliumlike ions. Its validity will be discussed below. We may include ion collisions. According to the method of the quasi-steady-state solution originally developed for hydrogen [2], the time derivative of the population of excited levels is set equal to 0, so that the set of coupled differential equations for the excited levels reduces to a set of coupled linear equations. The solution is expressed as the sum of the two terms,

$$n(p)=R_0(p)n_e n_{\mathrm{He}}+R_1(p)n_e n_{\mathrm{Li}}\ , \tag{2}$$

where $R_0(p)$ and $R_1(p)$ are the population coefficients which are functions of n_e and electron temperature T_e (and of ion density and temperature when we include ion collisions). The ground-state lithiumlike ion density, i.e., $n(2\,^2S)$, has been expressed as n_{Li}. The first term may be called the recombining plasma component, and the second term the ionizing plasma component [3].

We define the effective ionization rate coefficient (S_{eff}) and the recombination rate coefficient (α_{eff}) as

$$S_{\rm eff}=\frac{\sum_{p=1,2}\left[S(p)R_1(p)+\sum_{q\geq 3}C(p,q)R_1(p)-\sum_{q\geq 3}F(q,p)R_1(q)\right]}{[R_1(1)+R_1(2)]}\ ,$$
$$\alpha_{\rm eff}=\sum_{p=1,2}\left[\alpha(p)n_e+\beta(p)+\gamma(p)+\sum_{q\geq 3}F(q,p)R_0(q)n_e\right]\ , \tag{3}$$

where $p=1$ and 2 are understood to denote the ground state [$R_1(1)=1$] and $2p\ ^2P_{1,2,3/2}$, respectively. These are different from the collisional-radiative rate coefficients defined for hydrogen [2].

A. Collisional-radiative model with fine structure unresolved

In the case of a CR model with fine structure unresolved, we assume that the fine structure sublevels belonging to a level are populated according to their statistical weights. Let p in Eq. (1) represent the principal quantum number n and the angular momentum quantum number l, and $n(p)$ is the sum of the populations of the fine structure sublevels. Each of the rate coefficients in Eq. (1) refers to level p or q, and is expressed in terms of the rate coefficients for transitions connecting individual fine-structure sublevels as

$$B(p,q)=\frac{g(p_1)}{g(p)}\{B(p_1,q_1)+B(p_1,q_2)\}+\frac{g(p_2)}{g(p)}\{B(p_2,q_1)+B(p_2,q_2)\}\ , \tag{4}$$

where $B(p,q)$ stands for $C(p,q)$, $A(p,q)$, or $F(p,q)$, and p and q denote the initial and final levels, respectively. Here p_1 and p_2 are fine-structure sublevels with total angular momentum $j=l-\frac{1}{2}$ and $j=l+\frac{1}{2}$, respectively, and $g(p)$ is the statistical weight of level p. In the case of an S state, the p_1 or q_1 term is absent. The ionization and recombination rate coefficients are defined as

$$S(p)=\frac{g(p_1)}{g(p)}S(p_1)+\frac{g(p_2)}{g(p)}S(p_2) \tag{5a}$$
$$\alpha(p)=\alpha(p_1)+\alpha(p_2)\ , \tag{5b}$$

similarly for $\beta(p)$ or $\gamma(p)$.

B. Collisional-radiative model with fine structure resolved

When the nuclear charge z is large, a population imbalance may develop in the fine-structure sublevels. We introduce a quantity $\mu(p)$ which describes the population imbalance:

$$\mu(p)=\omega_1-\omega_2\ , \tag{6a}$$

with

$$\omega_1=\frac{n(p_1)}{g(p_1)},\quad \omega_2=\frac{n(p_2)}{g(p_2)}\ . \tag{6b}$$

In the case that the populations are distributed according to the statistical weights, μ is 0.

The quantity μ is given by a set of coupled equations, the details of which are described in the Appendix. According to the spirit of the CR model, the time derivative of μ is set equal to 0. The solution is described, with the help of Eq. (2), as

$$\mu(p)=\rho_0(p)n_e n_{\rm He}+\rho_1(p)n_e n_{\rm Li}\ . \tag{7}$$

When $\mu(p)$ is different from zero, the treatment presented in Sec. II A becomes inadequate, and correction terms are added to the right hand side of Eq. (1) as described in the Appendix.

III. ATOMIC PROCESSES

In this section, we use two kinds of notations to denote the levels; $n\ ^2L$ refers to a level with the fine structure unresolved, and $nl\ ^2L_{l\pm 1/2}$ refers to the fine-structure sublevels.

A. Energy level

The levels for $n\leq 5$ are treated separately according to their angular momentum quantum number l, and we may include the fine structure for these levels. For the CR model with the fine structure unresolved, we define the level energy by taking the weighted average of the energies of the fine-structure sublevels with their statistical weights. All the levels of $6\leq n\leq 40$ are treated as hydrogenic, and different l levels are bundled together.

The ionization potential of the ground state and the transition energy from the ground state to $n\leq 5$ levels are taken from Zhang, Sampson, and Fontes [4]. The ionization potential of these low-lying levels has an approximately $z_{\rm eff}^2$ dependence with $z_{\rm eff}=z-2$ (z is the nuclear charge), whereas the transition energies from the ground state to $2p\ ^2P_{1/2,3/2}$ have a $z_{\rm eff}^{+1}$ dependence for $z<15$.

B. Oscillator strength

We use the data of Zhang, Sampson, and Fontes [4] for transitions from the ground state and the $2p\ ^2P_{1/2,3/2}$ levels, and we use the data of Lindgard and Nielsen [5] for transitions from $n=3$, 4, and 5 levels. These data agree with those in the compilation by Wiese [6]. Figure 1 shows examples of the oscillator strengths for some transitions. Relativistic effects are seen for $z>20$.

We include an optically forbidden transition, $2p\ ^2P_{1/2}-2p\ ^2P_{3/2}$: the transition probability is given for $z=26$–36 [7], and scaled ($\propto z_{\rm eff}^{12}$) for other z ions.

C. Excitation cross section

For transitions $2s\ ^2S_{1/2}-2p\ ^2P_{1/2,3/2}$, $2s\ ^2S_{1/2}-3p\ ^2P_{1/2,3/2}$, and $2s\ ^2S_{1/2}-3s\ ^2S_{1/2}$, there are many theoretical, experimental, and semiempirical cross section data [4,8–13]. Comprehensive data for oxygen to

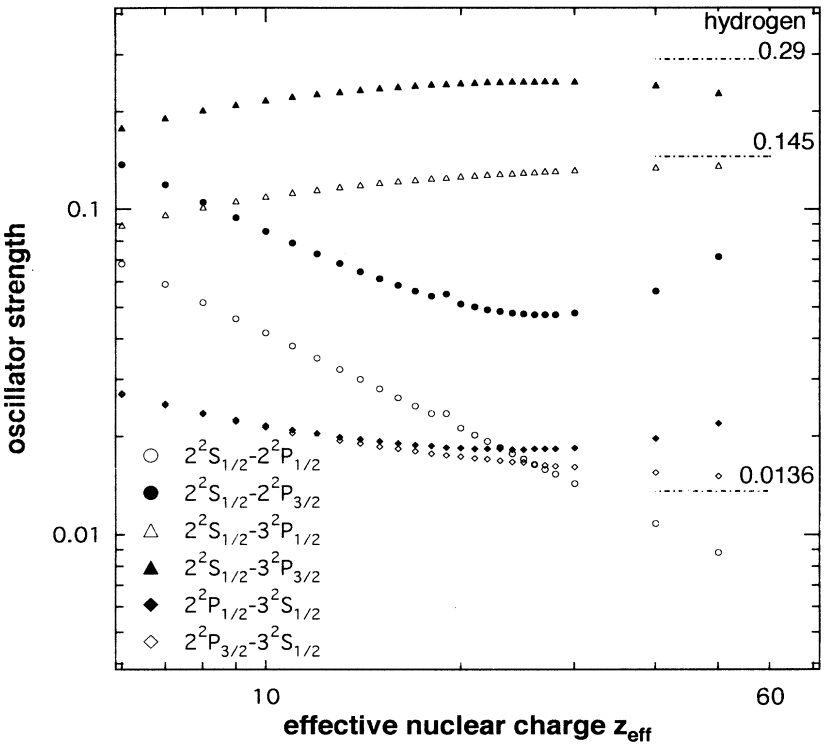

FIG. 1. z_{eff} dependence of the absorption oscillator strength for several transitions. Corresponding oscillator strength values for neutral hydrogen are given for the $n=2-n=3$ transitions.

uranium are given by Zhang, Sampson, and Fontes [4]. For transitions between excited levels or between the ground state and highly excited levels, however, there are few published data. We have calculated cross sections for virtually all transitions among the levels from $2s\ ^2S_{1/2}$ to $5g\ ^2G_{7/2,9/2}$ for the O VI ion. These cross section data are referred to as Clark, Csanak, and Abdallah (CCA), and details of the calculation method are given in [14].

Figure 2 shows the excitation cross section $2\ ^2S-3\ ^2P$ of O VI (optically allowed transition). Here the fine-structure-resolved data ([4] and CCA) have been reduced by Eq. (4) to the unresolved data shown. The results by Zhang, Sampson, and Fontes [4] and CCA are in good agreement. In the high energy range, the hydrogenic ap-

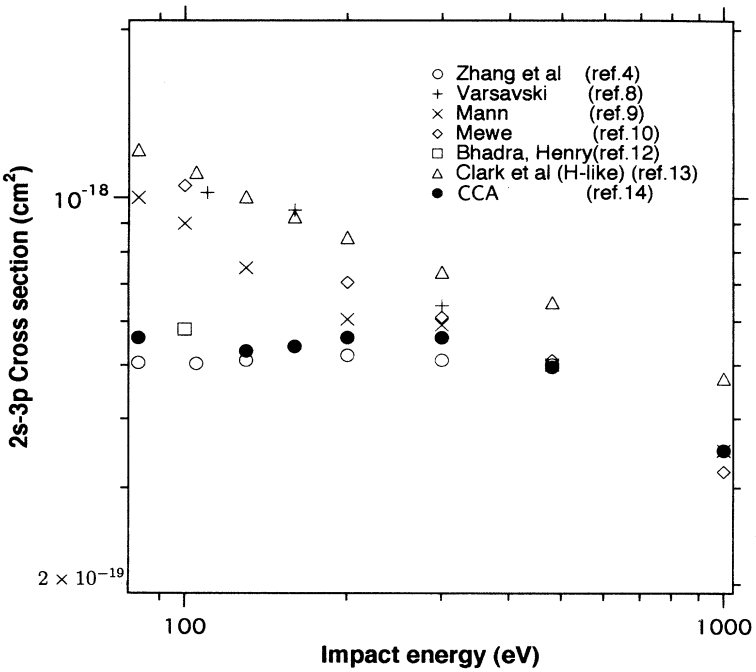

FIG. 2. Electron impact excitation cross section for $2\ ^2S-3\ ^2P$.

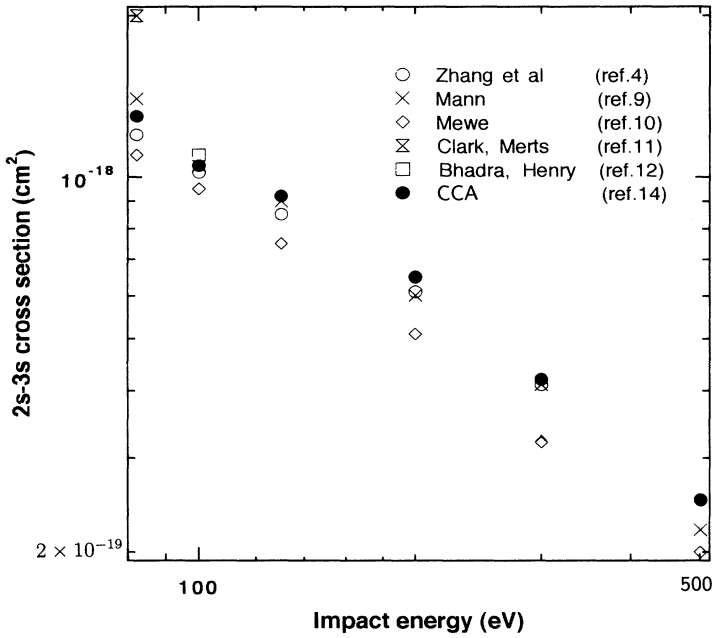

FIG. 3. Electron impact excitation cross section for $2\,^2S-3\,^2S$.

proximation by Clark, Sampson, and Goett [13] is larger by a factor 1.5. This difference may be attributed to the hydrogenic oscillator strength value, which is larger approximately by this amount (see Fig. 1).

For other lithiumlike ions with nuclear charge z, we use Zhang, Sampson, and Fonte's cross section data for transitions from the ground state and from $2p\,^2P_{1/2,3/2}$. For other transitions among the $n \leq 5$ levels, we adopt the following scaling formula:

$$\sigma(E/E_{\rm th})=\sigma_{\rm oxygen}(E/E_{\rm th})\left[\frac{Z-s}{8-s}\right]^{-4}\frac{f_z}{f_{\rm oxygen}}\,, \tag{8}$$

where $\sigma_{\rm oxygen}$ refers to the CCA cross section expressed in the threshold units $E/E_{\rm th}$, s is the screening constant given by Mayer [15] for the lower level, and f_z is the absorption oscillator strength for ion z.

Figure 3 shows the $2\,^2S-3\,^2S$ cross section (optically forbidden transition). All the cross sections agree well. For other z ions, we scale the data of Zhang, Sampson, and Fontes and CCA in a similar way to the optically allowed transition

$$\sigma(E/E_{\rm th})=\sigma_{\rm oxygen}(E/E_{\rm th})\left[\frac{Z-s}{8-s}\right]^{-4}. \tag{9}$$

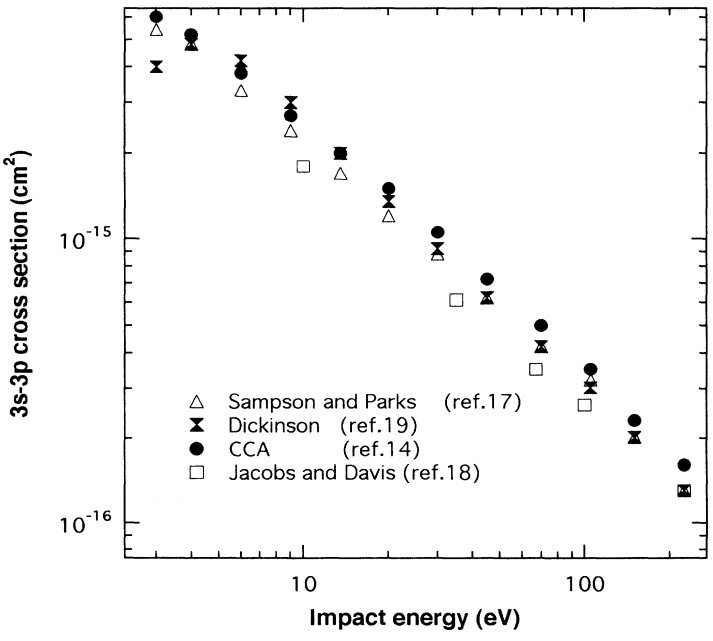

FIG. 4. Electron impact l-changing cross section for $3\,^2S-3\,^2P$. The results of Jacobs and Davis have been derived from their semiempirical l-changing rate coefficient.

For transitions from $n \leq 5$ to $n \geq 6$ levels, we scale the above excitation cross sections according to the threshold energies and the absorption oscillator strengths. For transitions between the excited levels of $n \geq 6$, we assume these to be hydrogenic, and choose the semiempirical cross section of Vriens and Smeets [16].

Figure 4 shows the $3\,^2S-3\,^2P$ excitation cross sections, taken as examples of the l-changing transitions. Results by CCA and Sampson and Parks [17] and semiempirical results by Jacobs and Davis [18] agree well. Also given is the cross section calculated from the formula originally derived by Dickinson [19] and generalized by Fujima [20]. In view of the good agreements even for these low-lying levels, we decided to use the latter formula for the l-changing transitions $l \leftrightarrow l+1$ between the levels with same n.

In many cases lithiumlike ions are observed as an impurity in, say, a tokamak hydrogen plasma. In these cases, the electron temperature is too high for the l-changing process to be effective (see Fig. 4). Rather, ion collisions may play a role. We include them when it is appropriate. The cross section $\sigma_z(v)$ for collisions by ions with an effective nuclear charge z is approximated by

$$\sigma_z(v)=z^2\sigma_e(v) \tag{10}$$

for higher energies, or collision speed $v > v_{eth}$, where $\sigma_e(v)$ is the cross section for electron collision, and v_{eth} is the threshold electron speed. For lower energies, the cross section is assumed to be proportional to v^2, as suggested from the comparison of $\sigma_1(v)$ and $\sigma_e(v)$ for neutral atoms [21] down to the threshold. In the case of proton collisions, the proton density and temperature are assumed to be equal to n_e and T_e, respectively.

D. Ionization cross section

Hofmann *et al.* [22] measured by a crossed beam technique the ionization cross section from the ground state for lithiumlike carbon, nitrogen, and oxygen ions, and showed that the contribution from the processes via doubly and triply excited levels are small. For $2\,^2S$ through $5\,^2G$ we use the hydrogenic approximation by Sampson and co-workers [23–28], which agree with the calculation of Kunc [29] and the semiempirical cross section of Lotz [30]. For $n \geq 6$ levels, we use the hydrogenic cross sections of Vriens and Smeets [16].

E. Recombination processes

Burgess [31] gives radiative recombination rate coefficients for hydrogenic ions, and MacLaughlin and Hahn [32] modify the results to nonhydrogenic ions. In the case of the lithiumlike ion, the free-bound oscillator strength of each level is rather close to that of hydrogen, and we use the calculation by Burgess, which is consistent with the total radiative recombination rate coefficient measured by Andersen and Bolko [33].

For dielectronic recombination, we include $2pnl$ and $3pnl$ ($n \geq 2$) as the intermediately doubly excited levels, and we use the autoionization and radiative decay probabilities given by Bely-Dubau *et al.* [34] for the O VI ion. For other z elements, we fit these quantities to calculation [35].

IV. CALCULATION RESULT AND COMPARISON WITH EXPERIMENT

We calculate population coefficients for various electron temperatures T_e and electron densities n_e. In many actual situations excited level populations [Eq. (2)] are given either by the ionizing plasma component or the recombining plasma component. In other words, depending on the particular plasma condition, the minor component could be negligibly small compared with the major component. We therefore discuss these components separately.

A. Populations of excited levels

The ionizing plasma component is proportional to the density of the ground-state ions. Figure 5 shows the n_e-dependence of the populations of some of the excited levels of O VI ions taken as an example, where the fine structure is unresolved. T_e is 50 eV and n_{Li} is 1 cm^{-3}, and we include proton collisions. We may express T_e and n_e by the reduced temperature Θ and density η,

$$\Theta=\frac{T_e}{z_{\mathrm{eff}}^2},\quad \eta=\frac{n_e}{z_{\mathrm{eff}}^7}\ . \tag{11}$$

These quantities are a measure of equivalent quantities for neutral species, $z_{\mathrm{eff}}=1$, i.e., neutral lithium, or even neutral hydrogen, the characteristics of which are well understood in plasma [3]. The plasma conditions in Fig. 5 corresponds to $\Theta=1.4$ eV and $\eta=3\times10^7$ cm^{-3} through 3×10^{15} cm^{-3}. When we neglect the proton collisions the n_e value at which the different l levels tend to each other are higher by factors 2, 5, and 30 for $n=3$, 4, and 5, respectively.

Figure 6 shows the recombining plasma component; we take the Al XI ion, and T_e is assumed to be 30 eV ($\Theta=0.25$ eV). Only the populations of the $n=3$, 4, and 5 levels are shown. For the purpose of the analysis in the following paper [36], we have included the effect of ion collisions ($z=10$), where we assume the ion density and temperature are 10% of n_e and equal to T_e, respectively.

B. The population imbalance in the fine structure sublevels

Figure 7 shows the degree of the population imbalance between the fine-structure sublevels of $2\,^2P_{1/2,3/2}$. The ordinate is the imbalance normalized to ±1, $\mu(p)/(\omega_1+\omega_2)$. We have assumed the ionizing plasma with $\Theta=3$ eV and $\eta=10^8$ cm^{-3} through 10^{16} cm^{-3}. The large imbalance for large nuclear charge ($z>20$) is due mainly to the difference in the radiative decay probabilities from the $2p\,^2P_{1/2,3/2}$ levels. In the high density regions, the imbalance disappears; this is because of the collisional depopulation to the $2s\,^2S_{1/2}$ level. A small imbalance remains even for small z. The $3p\,^2P_{1/2,3/2}$ and higher levels show very small imbalance throughout the electron density region for $z \leq 40$.

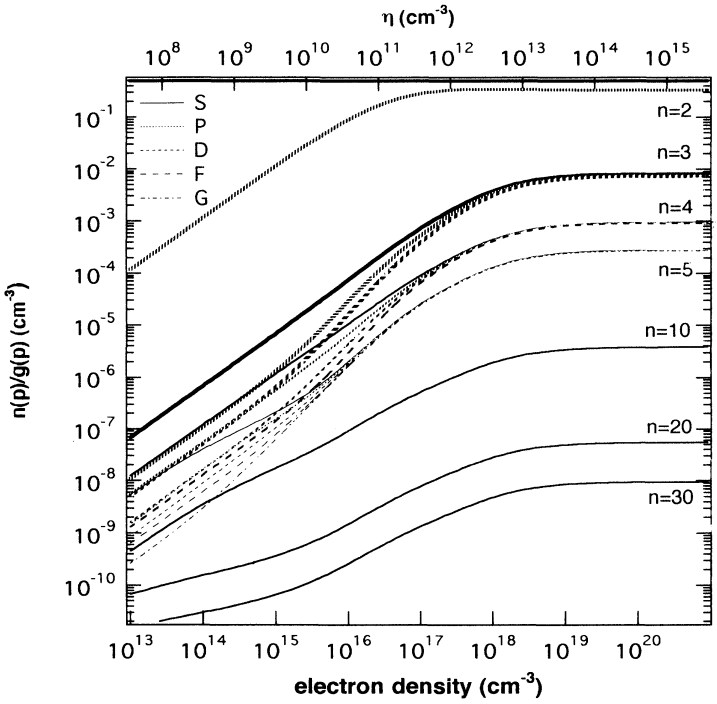

FIG. 5. The ionizing plasma component of the excited level populations of O VI ions (O^{5+}). $n(2\,^2S)$ and T_e are assumed to be 1 cm^{-3} and 50 eV, respectively. Proton (ion) collisions are included.

C. Comparison with experiments

Several plasma experiments have been reported which are relevant to the present calculation.

Datla and Kunze [37] measured spectral line intensities from O VI and N V ions in a theta pinch plasma. They define the effective rate coefficient as

$$X_{\text{eff}}(p)=\frac{n(p)\sum_{q<p}A(p,q)}{n_e[n(2\,^2S)+n(2\,^2P)]} \tag{12}$$

and present several X_{eff}'s normalized by $X_{\text{eff}}(3\,^2S)$. They regard $[n(2\,^2S)+n(2\,^2P)]$ as the lithiumlike ion density.

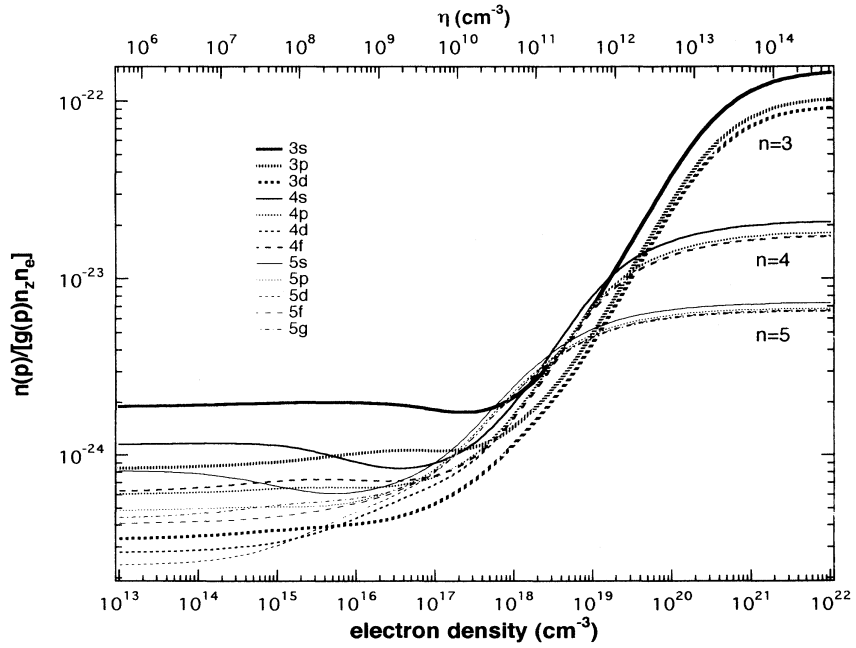

FIG. 6. The recombining plasma component of the excited level populations of Al XI ions (Al^{10+}). T_e is assumed to be 30 eV. Ion collisions are included.

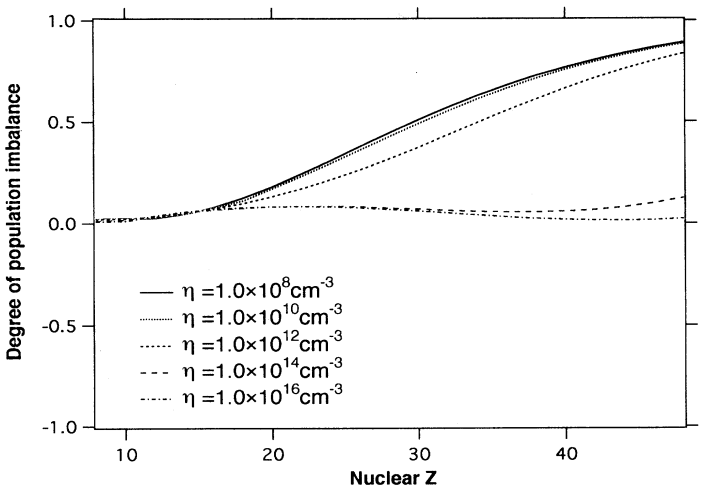

FIG. 7. z dependence of the population imbalance between the $2p\ ^2P_{1/2}$ and $2p\ ^2P_{3/2}$ levels for several reduced electron densities.

The population ratio $\beta = n(2\,^2P)/n(2\,^2S)$ is calculated by Sampson to be 0.88 for N V and 0.58 for O VI. Table I reproduces the result. Their plasmas for N V and O VI ions happen to have nearly the same Θ and an identical η. As seen from Fig. 5, at this density, these levels, especially the $n=5$ levels, are not in the corona phase [3]. Rather, the density effects, i.e., population contributions from excited levels, are appreciable or even dominant (see the last columns in Table I; see also [36]). The density effects are minimal for $3\,^2S$, and its excitation cross section from $2\,^2S$ has small uncertainties (Fig. 3). It is judged that the choice of this level as the denominator for normalization is suitable. By using Eq. (12) we reinterpret the result and retrieve the population ratio. Figure 8 compares experimental relative populations of excited levels of O VI and N V ions and the calculated ones. It is noted that the curves for O VI is nothing but a reproduction of Fig. 5. Our results agree with the experimental results within the experimental uncertainties except for $3\,^2D$ of O VI; for this level the experimental population is smaller by a factor 1.9. For N V ions, the discrepancy is in the same direction but its magnitude is smaller. For $3\,^2P$ and $4\,^2P$, the experimental results are larger than our results in the case of N V ions, and smaller in the case of

TABLE I. Relative effective excitation rate coefficient ($cm^3\ s^{-1}$). Comparison of the rate coefficients of the experiment [37] and the present calculation. The last three columns show the relative contributions from the population flows from various levels. β is the ratio of the population of $n(2\,^2P)$ and $n(2\,^2S)$, i.e., $\beta = n(2\,^2P)/n(2\,^2S)$. β_{SP} is the result of Sampson and Parks [17]. The numbers in brackets denote multiplicative powers of 10.

T_e (eV)	n_e (cm^{-3})	Level	Datla and Kunze [37]	β_{SP} $[n(2P)/n(2S)]$	Present	β_{ours}	Contribution (%) 2S	2P	l-changing
				N V					
		5D	0.14		0.17		2	5	92
		5P	0.06		0.05		2	2	95
45	5.5 [15]	4D	0.58		0.70		11	27	59
		4P	0.22		0.28		18	11	69
		4S	0.13	0.88	0.10	0.62	21	27	49
$\Theta=1.8$	$\eta=7.0$ [10]	3D	3.7		5.3		22	68	7
		3P	1.4		1.8		25	43	30
		3S	1		1		57	24	17
				O VI					
		5D	0.15		0.14		2	6	92
		5P	0.06		0.05		1	2	96
50	2.0 [16]	4D	0.96		0.68		11	30	56
		4P	0.34		0.28		15	15	66
		4S	0.08	0.54	0.09	0.77	21	27	48
$\Theta=1.4$	$\eta=7.0$ [10]	3D	5.02		6.3		20	71	6
		3P	2.75		2.1		18	54	25
		3S	1		1		58	24	16

TABLE II. Effective ionization rate coefficient ($cm^3 s^{-1}$). Comparison of the rate coefficients between the several experimental results and the present calculation. The last column shows the relative contriubtion from the ladderlike excitation-ionization process. An uncertainty labeled *b* means that the measurement is accurate within a factor of 2.

Ion	Ref.	T_e (eV)	n_e (cm^{-3})	Experiments	Present	Indirect (%)
C IV	38	120	3.0[15]	1.3±*b*[−9]	3.2[−9]	38
N V	41	80	4.0[15]	7.4±2.2[−10]	8.8[−10]	35
N V	40	100	1.0[16]	9.7±2.9[−10]	1.2[−9]	43
N V	38	188	4.0[15]	5.9±*b*[−10]	1.5[−9]	27
O VI	43	55	2.5[16]	1.4±0.3[−10]	1.6[−10]	55
O VI	41	80	4.0[15]	4.1±1.2[−10]	2.7[−10]	29
O VI	40	110	1.8[16]	3.9±1.2[−10]	5.0[−10]	40
O VI	40	120	1.4[16]	4.4±1.3[−10]	5.6[−10]	36
O VI	38	200	4.0[15]	3.4±*b*[−10]	6.9[−10]	20
Ne VIII	42	65	6.0[12]	1.4±0.7[−11]	9.1[−12]	3
Ne VIII	39	230	1.0[16]	1.1±0.4[−10]	2.0[−10]	17

O VI.

In order for our calculated $3\,^2D$ population of O VI ions to be consistent with the experiment, the *l*-changing cross section should be decreased at least by one order. It may be interesting to note that if the experimental n_e for O VI were reduced by a factor 2 or 3, the experimental population would be in almost complete agreement with the calculation except for levels $4\,^2S$ and $5\,^2P$.

Ionization rate coefficients of lithiumlike ions are measured by Kunze [38], Jones and co-workers [39,40], Rowan and Roberts [41], Hinnov [42], and Datla and Roberts [43] in theta pinch plasmas. These results are summarized in Table II, where they are compared with the effective ionization rate coefficient S_{eff} defined by Eq.

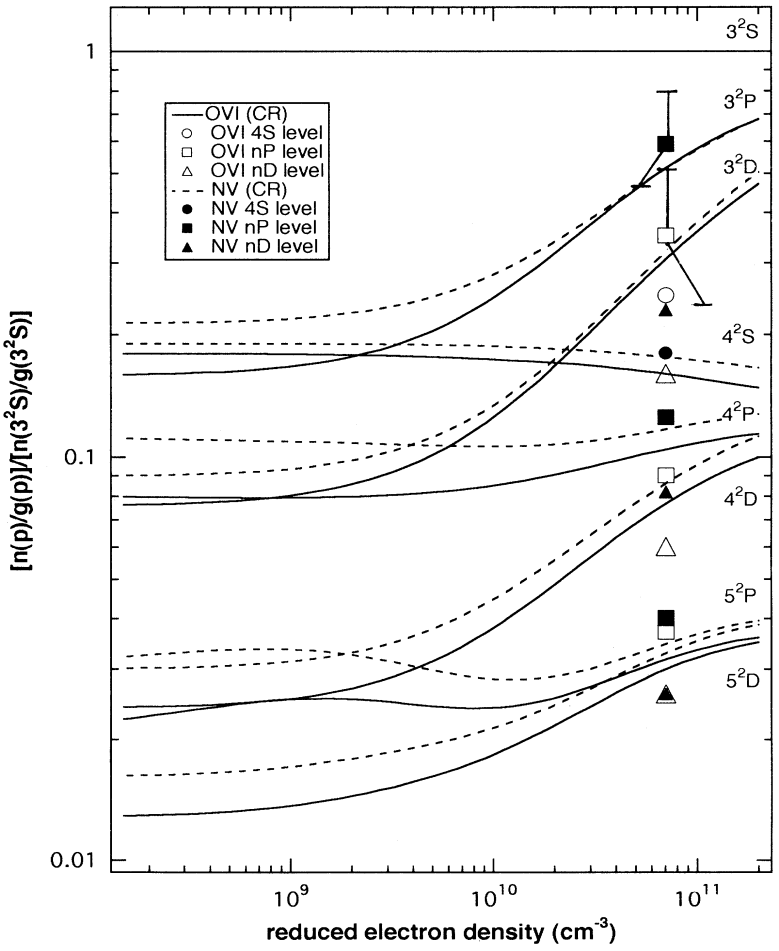

FIG. 8. Comparison of the relative population of several excited levels of O VI and N V ions in ionizing plasma with the experimental results by Datla and Kunze [37]. O VI and N V populations are expressed by the open and closed symbols, respectively. The plasma conditions are referred to in Table I.

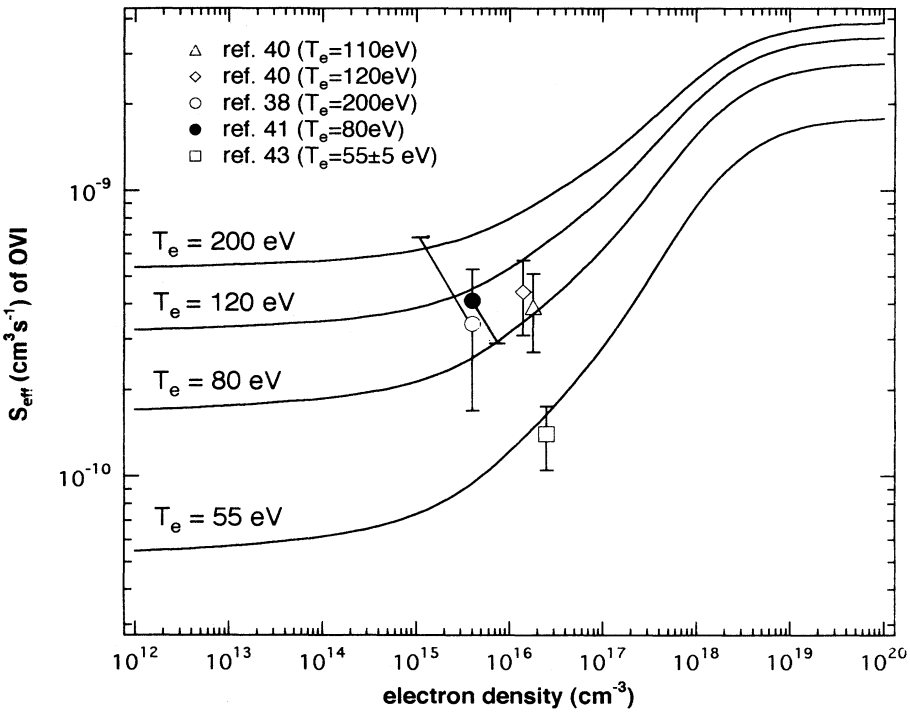

FIG. 9. The n_e dependence of S_{eff} of O VI for several temperatures. Experimental results are compared.

(3), which includes indirect ionization through the excited levels (the ladderlike process [3]). The experimental results of [40] and [43] are in agreement with our calculation within experimental uncertainties. Reference [41] for O VI gives larger values, while [41] for N V agrees with our calculation. References [38] and [39] give smaller values; especially [38], although with a large uncertainty of a factor 2, gives consistently smaller values for C IV, N V, and O VI ions. Figure 9 summarizes the comparison for O VI. It is noted that the experimental ionization rate coefficient of [38] is even smaller than the low density limit value, or the direct ionization rate coefficient.

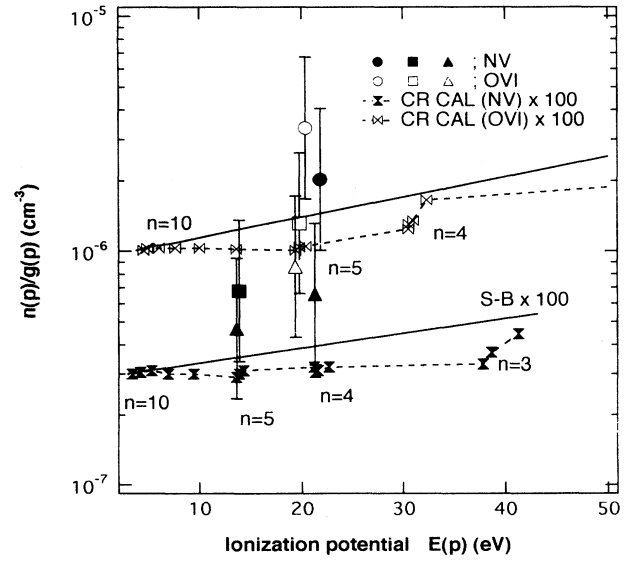

FIG. 10. Comparison of the calculated population of several levels of O VI and N V ions in recombining plasma with the experimental results by Datla and Kunze [37] in Boltzmann plots. The calculation results has been multiplied by a factor 100.

There are few experiments available for comparison of the recombination processes. Datla and Kunze [37] report the effective recombination rate coefficients $\alpha_{\text{eff}}(p)$ for the $n=4$ and 5 excited levels in the theta pinch plasma for O VI and N V ions. Figure 6 shows that the conditions of their experiment, ($n_e=2.5\times10^{16}$ cm^{-3} ($\eta=0.9\times10^{11}$ cm^{-3}) for O VI and $n_e=1.0\times10^{16}$ cm^{-3} ($\eta=1.4\times10^{11}$ cm^{-3}) for N V) are in the intermediate toward high density regions for $n=4$ and, especially, 5. Thus the assumption that the population of the individual levels is determined by the balance between recombination and radiative and collisional decay is clearly inappropriate. It is also seen that the levels with $n=4$ and 5 are almost statistically populated. (See the following paper for details.) We retrieve the experimental populations from their $\alpha_{\text{eff}}(p)$ values, where the heliumlike ion density $n_{\text{He}}=1$ cm^{-3} is assumed for convenience of presentation. We compare in Fig. 10 the experimental and theoretical populations in the Boltzmann plot. The discrepancies between our results and experiment are about two orders of magnitude. It may be unrealistic to try to bring our calculation into agreement with the experiment by introducing an additional recombination process, because these levels, especially $n=5$, are almost in local thermodynamic equilibrium (LTE) with respect to the heliumlike ions.

V. UNCERTAINTIES AND VALIDITY RANGE

A. Atomic data

The uncertainty in the level energy calculated by Zhang, Sampson, and Fontes [4] is claimed to be less than 1%. The uncertainty due to the fitting formula adopted in this study is less than 0.5%.

The uncertainty in the absorption oscillator strength data of Zhang, Sampson, and Fontes [4] is about 1%, and that of Lindgard and Nielsen [5] is about 1% for $z \leq 18$, and within 10% for $z \geq 20$. The uncertainty due to the fitting formula is less than 5%. The resulting uncertainty in the A coefficient for the transitions into $n=3$, 4, and 5 levels is 10% in the case of high-z ions. The irregularity of the $2s\,^2S_{1/2}-2p\,^2P_{1/2,3/2}$ absorption oscillator strengths at $z=21$ seen in Fig. 1 is ignored in our computer code.

The results of various calculations, except for the hydrogenic approximation [4, 8–12 and 14], for the excitation cross section of O VI are in good agreement for all transitions except for $2\,^2S-3\,^2P$ (see Figs. 2–4). For this transition, the cross section of Mann is larger than those of CCA and Zhang, Sampson, and Fontes by a factor 2 near the threshold (Fig. 2). If we adopt the former cross section, the resulting population of the $3\,^2P$ level changes appreciably in low temperature regions.

B. Validity of Eq. (2)

In Eqs. (1) and (2), we have assumed that production of excited ions directly from the berylliumlike ions is insignificant; that it, its flow is less than, say, 10% of the contributions given in the right hand side of Eq. (1). We take O VI as an example. In the low density region ($\eta \leq 10^7$ cm^{-3}), where the excited level populations of berylliumlike ions are low, the ionization-excitation process from $2s^2\,^1S$ to $n\,^2L$ must be considered; the ratio of these rate coefficients to those for $2s\,^2S$ to $n\,^2L$ is estimated to be of the order of 10^{-5}. Thus a conservative estimate leads to a condition $n_{\rm Be}/n_{\rm Li} < 10^2 \sim 10^3$. In the region of 10^7 cm^{-3} $< \eta < 10^{12}$ cm^{-3}, the ratio of the metastable $2s2p\,^3P$ population to the ground-state population is 0.3 [44]. From the comparison of ionization of $2s2p\,^3P$ creating $2\,^2P$ and excitation $2\,^2S-2\,^2P$, it is concluded that $n_{\rm Be}/n_{\rm Li} < 20$ should be satisfied. In the high density limit ($\eta > 10^{12}$ cm^{-3}), the ladderlike excitation-ionization mechanism through the $2snl$ and $2pnl$ Rydberg states may create the $2\,^2S$ and $2\,^2P$ ions, respectively. The ratio of the production rate of $2\,^2P$ to that of $2\,^2S$ is estimated to be 0.9. [In Eq. (1) we have assumed this to be zero.] In the extreme case that only $2\,^2P$ ions were created, all populations in Fig. 5 except or $n(2\,^2S)$ would be shifted by 20% upward, and $S_{\rm eff}$ in Fig. 9 would increase by 10%.

C. Assumption of hydrogenic approximation and statistical distribution for $n \geq 6$ levels

We assume the hydrogenic approximation for the $n \geq 6$ levels. As the nuclear z becomes large, quantum defects of excited levels become small. For lithiumlike ions with $z \geq 6$, the quantum defects of the $n \geq 6$ levels are smaller than 0.05, and this approximation may be justified.

For levels with $n \geq 6$, we assume that all the different l levels are populated according to their statistical weights. As we show in Figs. 5 and 6, in the low density region the populations of the different l levels for $n=3$, 4, and 5 largely deviate from the statistical distributions. A similar deviation is expected for the $n \geq 6$ levels in corresponding density regions. For the purpose of estimating errors in the populations of low-lying levels caused from our assumption for the $n \geq 6$ levels, we compare the results of a calculation in which the $n=5$ levels are assumed to be statistically populated. For an ionizing plasma of low density, this population is close to that of $5\,^2P$ in Fig. 5. In this case, the $4\,^2P$ population is smaller by 10%, and the $4\,^2F$ population, which is affected most, is larger by 20%. These charges are due to the lower $5\,^2S$ population and the enhanced $5\,^2G$ population, respectively, in this calculation. In a recombining plasma, the statistical population is close to $5\,^2G$ in Fig. 6. The discrepancy of the $4\,^2F$ population, which is affected most, is smaller (2%), because the $5\,^2G$ population does not change substantially between the two calculations. The populations of the $n=3$ and 2 levels are little affected for both the ionizing and recombining plasmas. Judging from the above observations, we may conclude that, in our present model, the $n=5$ levels are, in low density regions, overpopulated at most by 20% for $5\,^2G$ in the ionizing plasma, and reasonably accurate in the recombining plasma. The populations of the $n=4$, 3, and 2 levels are little affected by our assumption. Our assumption would be substantiated in the high density region where the l-changing collisions are frequent enough for the $n=6$ levels. The critical density would be given from a comparison of the radiative decay rate and the l-changing collisional rate of $6\,^2D$. In the case that proton collisions are neglected, the critical density is $n_e \cong 5\times 10^{16}$ cm^{-3} for the condition of Fig. 5, and in the case that proton collisions are included the critical density is $n_e \cong 1\times 10^{15}$ cm^{-3}.

ACKNOWLEDGMENT

The calculation of excitation cross section by CCA was performed under the auspices of the U.S. Department of Energy.

APPENDIX

The population imbalance $\mu(p)$ is described by the coupled equation

$$\frac{d\mu(p)}{dt}=\left[\sum_{q<p}C'(q,p)n_e+\sum_{q>p}\{F'(q,p)n_e+A'(q,p)\}\right]n(q)$$
$$-\left[\sum_{q<p}\{F''(p,q)n_e+A''(p,q)\}+\sum_{q>p}C''(p,q)n_e+S''(p)n_e\right]n(p)$$
$$+\left[\sum_{q<p}K(q,p)n_e+\sum_{q>p}\{M(q,p)n_e+U(q,p)\}\right]\mu(q)$$
$$-\left[\sum_{q<p}\{M(p,q)n_e+U(p,q)\}+\left\{\sum_{q>p}K(p,q)+I(p)+V(p)\right\}n_e+A(p)\right]\mu(p)$$
$$+\{\alpha'(p)n_e+\beta'(p)+\gamma'(p)\}n_e n_{\mathrm{He}}\ , \tag{A1}$$

where $C'(q,p)$, $F'(q,p)$, and $A'(q,p)$ are the imbalance creation rate coefficients in level p from population of another level q by collisional excitation, deexcitation, and radiative decay, respectively, and they are defined as follows:

$$B'(q,p)=\frac{g(q_1)}{g(q)}\left\{\frac{B(q_1,p_1)}{g(p_1)}-\frac{B(q_1,p_2)}{g(p_2)}\right\}$$
$$+\frac{g(q_2)}{g(q)}\left\{\frac{B(q_2,p_1)}{g(p_1)}-\frac{B(q_2,p_2)}{g(p_2)}\right\}. \tag{A2}$$

$C''(q,p)$, $F''(q,p)$, and $A''(q,p)$ are the rate coefficients for imbalance destruction or creation in level p by depopulation, and they are defined as

$$B''(p,q)=\frac{1}{g(p)}\{B(p_1,q_1)+B(p_1,q_2)$$
$$-B(p_2,q_1)-B(p_2,q_2)\} \tag{A3}$$

and

$$S''(p)=\frac{1}{g(p)}[S(p_1)-S(p_2)]\ . \tag{A4}$$

$K(q,p)$, $M(q,p)$, and $U(q,p)$ are the imbalance transfer rate coefficients from levels q to p by excitation, deexcitation, and radiative decay, respectively, and

$$B(q,p)=\frac{g(q_1)g(q_2)}{g(q)}\left\{\frac{B(q_1,p_1)}{g(p_1)}-\frac{B(q_1,p_2)}{g(p_2)}-\frac{B(q_2,p_1)}{g(p_1)}+\frac{B(q_2,p_2)}{g(p_2)}\right\}. \tag{A5}$$

The imbalance in p is decreased by the depopulation processes

$$B(p,q)=\frac{g(p_1)g(p_2)}{g(p)}\left\{\frac{B(p_1,q_1)}{g(p_1)}+\frac{B(p_1,q_2)}{g(p_1)}+\frac{B(p_2,q_1)}{g(p_2)}+\frac{B(p_2,q_2)}{g(p_2)}\right\}. \tag{A6}$$

$I(p)$ is the imbalance destruction rate coefficient by ionization, and $\alpha'(p)$, $\beta'(p)$, and $\gamma'(p)$ are the imbalance creation rate coefficients by recombination. These are defined as

$$I(p)=\frac{g(p_1)g(p_2)}{g(p)}\left\{\frac{S(p_1)}{g(p_1)}+\frac{S(p_2)}{g(p_2)}\right\},$$
$$\alpha'(p)=\left[\frac{\alpha(p_1)}{g(p_1)}-\frac{\alpha(p_2)}{g(p_2)}\right], \tag{A7}$$

and similarly for $\beta'(p)$ and $\gamma'(p)$. $A(p)$ and $V(p)$ are the radiative and collisional j-changing rate coefficients between the fine-structure sublevels of level p.

Equation (1) is modified by the correction terms

$$\frac{dn(p)}{dt}=\sum_{q<p}C(q,p)n_e n(q)-\sum_{q<p}[F(p,q)n_e+A(p,q)]n(p)$$
$$-\sum_{q<p}C(p,q)n_e n(p)+\sum_{q<p}[F(q,p)n_e+A(q,p)]n(q)$$
$$-S(p)n_e n(p)+[\alpha(p)n_e+\beta(p)+\gamma(p)]n_e n_{\mathrm{He}}$$
$$+\sum_{q<p}C'''(q,p)n_e\mu(q)-\sum_{q<p}[F'''(p,q)n_e+A'''(p,q)]\mu(p)$$
$$-\sum_{q<p}C'''(p,q)n_e\mu(p)+\sum_{q<p}[F'''(q,p)n_e+A'''(q,p)]\mu(q)-S'''(p)\mu(p)\ . \tag{A8}$$

Triple primed terms are the correction terms due to the imbalance of the populations of other excited levels, and the rate coefficients are defined as

$$B'''(q,p)=[B(p_1,q_1)+B(p_1,q_2)+B(p_2,q_1)+B(p_2,q_2)] . \quad \text{(A9)}$$

[1] A. Klisnick, A. Sureau, H. Guennou, C. Moller, and J. Virmont, Apply Phys. B **50**, 153 (1990).

[2] D. R. Bates, A. E. Kingston, and R. W. P. McWhirter, Proc. R. Soc. London **267**, 297 (1962); D. R. Bates and A. E. Kingston, Planet. Space Sci. **11**, 1 (1963); R. W. P. McWhirter and A. G. Hearn, Proc. Phys. Soc. **82**, 641 (1963).

[3] T. Fujimoto, J. Phys. Soc. Jpn. **47**, 265 (1979); **47**, 273 (1979); **49**, 1561 (1980); **49**, 1569 (1980); **54**, 2905 (1985).

[4] H. L. Zhang, D. H. Sampson, and C. J. Fontes, At. Data Nucl. Data Tables **44**, 31 (1990).

[5] A. Lindgard and S. E. Nielsen, At. Data Nucl. Data Tables **19**, 533 (1977).

[6] W. L. Wiese, M. W. Smith, and B. M. Glennon, Natl. Bur. Stand. Ref. Data Ser., Natl. Bur. Stand. (U.S.) Circ. No. 110 (U.S. GPO, Washington, D.C., 1966), Vol. 4.

[7] V. Kaufman and J. Sugar, J. Phys. Chem. Ref. Data **15**, 321 (1986).

[8] C. M. Varsavski, Planet. Space Sci. **11**, 1001 (1963).

[9] J. B. Mann (unpublished).

[10] R. Mewe, Astron. Astrophys. **20**, 215 (1972).

[11] R. E. H. Clark, A. L. Merts, J. B. Mann, and L. A. Collins, Phys. Rev. A **27**, 1812 (1983).

[12] K. Bhadra and R. J. W. Henry, Phys. Rev. A **26**, 1848 (1982).

[13] R. E. H. Clark, D. H. Sampson, and S. J. Goett, Astrophys. J. Suppl. **49**, 545 (1982).

[14] R. E. H. Clark, G. Csanak, and J. Abdallah, Jr., Phys. Rev. A **44**, 2874 (1991).

[15] H. Mayer, Los Alamos Scientific Laboratory Report No. LA-607 (1947) (unpublished).

[16] L. Vriens and A. H. M. Smeets, Phys. Rev. A **22**, 940 (1980).

[17] D. H. Sampson and A. D. Parks, Astrophys. J. Suppl. **28**, 263 (1974); **28**, 323 (1974).

[18] V. L. Jacobs and J. Davis, Phys. Rev. A **18**, 697 (1978).

[19] A. S. Dickinson, Astron. Astrophys. **100**, 302 (1981).

[20] K. Fujima (private communication).

[21] F. Aumayr, G. Lakits, and H. Winter, Z. Phys. D **6**, 145 (1987).

[22] G. Hofmann, A. Muller, K. Tinschert, and E. Salzborn, Z. Phys. D **16**, 113 (1990).

[23] L. B. Golden and D. H. Sampson, J. Phys. B **10**, 2229 (1977).

[24] L. B. Golden, D. H. Sampson, and K. Omidvar, J. Phys. B **11**, 3235 (1978).

[25] D. L. Moore, L. B. Golden, and D. H. Sampson, J. Phys. B **13**, 385 (1980).

[26] D. H. Sampson and L. B. Golden, J. Phys. B **12**, L785 (1979).

[27] L. B. Golden and D. H. Sampson, J. Phys. B **13**, 2645 (1980).

[28] R. E. H. Clark and D. H. Sampson, J. Phys. B **17**, 3311 (1984).

[29] J. A. Kunc, J. Phys. B **13**, 587 (1980).

[30] W. Lotz, Astrophys. J. Suppl. **14**, 207 (1967).

[31] A. Burgess, Mem. R. Astron. Soc. **69**, 1 (1964).

[32] D. J. MacLaughlin and Y. Hahn, Phys. Rev. A **43**, 1313 (1991); **45**, 5317(E) (1992).

[33] L. H. Andersen and J. Bolko, J. Phys. B **23**, 3167 (1990).

[34] F. Bely-Dubau, J. Dubau, P. Faucher, and L. Steenman-Clark, J. Phys. B **14**, 3313 (1981).

[35] L. A. Vainshtein and U. I. Safronova, At. Data Nucl. Data Tables **21**, 49 (1978).

[36] T. Kawachi and T. Fujimoto, following paper, Phys. Rev. E **51**, 1440 (1995).

[37] R. U. Datla and H. J. Kunze, Phys. Rev. A **37**, 4614 (1988).

[38] H.-J. Kunze, Phys. Rev. A **3**, 937 (1971).

[39] L. A. Jones, E. Källne, and D. B. Thomson, J. Phys. B **10**, 187 (1977).

[40] E. Källne and L. A. Jones, J. Phys. B **10**, 3637 (1977).

[41] W. L. Rowan and J. R. Roberts, Phys. Rev. A **19**, 90 (1979).

[42] E. Hinnov, J. Opt. Soc. Am. **56**, 1179 (1966); **57**, 1392 (1967).

[43] R. U. Datla and J. R. Roberts, Phys. Rev. A **28**, 2201 (1983).

[44] T. Kato, J. Lang, and K. E. Berrington, Nagoya Report No. NIFS-DATA-2 (1990) (unpublished).